RESERVOIR AND HYDROCARBON MAPPING USING FAR-OFFSET AND EXTENDED ELASTIC IMPEDANCE SEISMIC VOLUMES, WESTERN BASIN, GULF OF THAILAND

Devi Gasiani*

Petroleum Geoscience Program, Department of Geology, Faculty of Science,
Chulalongkorn University, Bangkok 10330, Thailand
*Corresponding author email: d.gasiani@gmail.com

Abstract

The study area lies in the center part of the Western Basin, Gulf of Thailand. The reservoirs in the study area are Middle Miocene sandstones of a fluvial-coastal depositional system. Mapping these types of reservoirs is known to be challenging due to rapid lateral variations and possibly complex extensional fault systems. Seismic imaging of these reservoirs using only full-stacked data still have some limitations near the study area. Therefore, rock physics analysis, post-stack seismic inversion and seismic attributes were applied using partial-angle stacked seismic data in order to map sand geometries and identify hydrocarbon-bearing zones. The rock physics analysis such as density, S-wave velocity, P-impedance, and elastic impedance cross plots show different trends of sand and shale along the well respectively. The impedance value of sand is lower than shale. The P-impedance and near-angle elastic impedance cannot distinguish clearly sand and shale lithology in the study area. However, the far-angle elastic impedance displayed a strong contrast of sand and shale trend, which can help identify lithology. The main reservoir Sand Aand secondary reservoir Sand B were observed by using the inverted volumes and seismic attributes such as RMS amplitude and sweetness. The extracted far-angle elastic impedance on vertical section along inverted elastic impedance volume may successfully map the oil-bearing sand. The RMS and sweetness attributes of the far-angle stacked volume show a stronger high amplitude contrast than near-angle and very far-angle stacked volumes. Thus, the combination of seismic attributes and inversion may successfully map reservoir distribution. This study suggests that far-angle elastic impedance can be used to map reservoir distribution and predict oil bearing-sands.

Keywords: Elastic impedance, Inversion, Seismic attributes, Partial-angle stacked seismic

1. Introduction

There are many challenges facing an attempt to map reservoirs in the Tertiary basins of the Gulf of Thailand using geophysical applications. The study area is situated in the center part of Western Basin of the Gulf of Thailand at a water depth of 60 m. Typical reservoirs in the study area are fluvial sands, which have lithological variations in both the lateral and vertical directions. Moreover, the north–south trending, normal fault system makes this basin to be highly compartmentalized. Therefore, prediction of reservoir distribution in this area is highly important. The well log data from 11 exploration wells in the study area were applied along with the partial-angle stacked seismic data in order to perform elastic impedance inversion.

P-Impedance and elastic impedance inversion for reservoir characterization were studied in the northern part of Pattani Basin by Kamolsilp (2016) and southern part by Tang-On (2018). Kamolsilp (2016) suggested that full-stack seismic volume often is not enough to preserve information about rock properties such as lithology and fluid, and the computed P-impedance has a limitation in differentiating the sand and shale. However, Kamolsilp (2016) also found that reservoir distribution and possible hydrocarbon zones can be identified using the far-angle elastic impedance inverted volume. The study by Tang-On (2018) discovered that in some cases, P-Impedance and 10˚-, 20˚-, and 30˚-elastic impedance volumes can be used to identify oil-bearing reservoirs. However, Tang-On (2018) found that 40˚-elastic impedance inverted volume is not appropriate to use in the data set since it has the least match with the blind test well.

The uncertainty in lithology and fluid identification based only on normal incidence

impedance can often be effectively removed by adding information about elastic properties such as shear wave and angle of incidence. The far-offset stack gives an estimate of a Vp/Vs related elastic impedance (EI) attribute, equivalent to the acoustic impedance for non-normal incidence (Mukerji et al., 1998). In the study area, there has not been any previously published result related to the elastic impedance in the Western Basin. Therefore, the elastic impedance inversions at near-, far and very far-angles (from incidence angle between 10 to 50 degrees) were completed to define the reservoirs.

2. Objectives

The aims of this study are to determine reservoir distribution and discriminate lithology and fluid within the reservoirs by using rock physics parameters and integration of elastic properties.

3. Study Area

The study area is situated in the Western Basin, located to the north-west of the main Pattani Trough, Gulf of Thailand (Figure 1). The Western Basin is a Tertiary age basin that contains more than 3000-meter thickness of Cenozoic clastic sediments in its deepest part (Lain and Bradley, 1987), overlying a basement comprising Permian Ratburi Group carbonates and Mesozoic intrusive and possibly the Jurassic Khlong Min Formation. The earliest date of basin inception is Oligocene and the movement along the major fault essentially resulted in a series of North-South oriented, extensional grabens and half-grabens. Regionally the area was affected by trans-tensional movement during the late Miocene (Khanna et al., 2013). Based on the well log interpretations, stratigraphic and structural correlation, the lithostratigraphy of the study area was summarized schematically into 4 main events by Khanna et al., 2013.

The Pre-Tertiary Sequence consists of Permian Ratburi group carbonates. These karstified carbonates are found to be productive at Nang Nuan field in the Chumphon Basin (Heward et al., 2000). The Syn-Rift Sequence consists of Late Oligocene to Early Miocene syn-rift megasequence of source-prone lacustrine shales and fluvio-deltaic sandstones and possibly lacustrine turbidite sandstones. The Post Rift Sequence comprised of Mid Miocene predominantly fluvial clastics with occasional marine mudstone and sandstone. The sands within Sequence T4 are the primary producing reservoir in the study area. The overlying formation containing sandstones was also found to be hydrocarbon bearing in the study area. The Mid-Miocene unconformity is poorly expressed in the working area. It does however appear to mark a boundary between non-hydrocarbon reservoir above and potential hydrocarbon reservoir below. The Post Rift Sequence II consists of Late Miocene to recent fluvial deposits with significant marine incursions.

This study focuses particularly on two sand units, Sand A which are in Sequence T4 and Sand B which are in Sequence T5. These reservoirs were deposited in a fluvial-coastal system in the post-rift Sequence. The type of reservoir is sandstones and the main production hydrocarbon products are oil. The gross thickness of these reservoirs ranges from 13 to 44 meters.

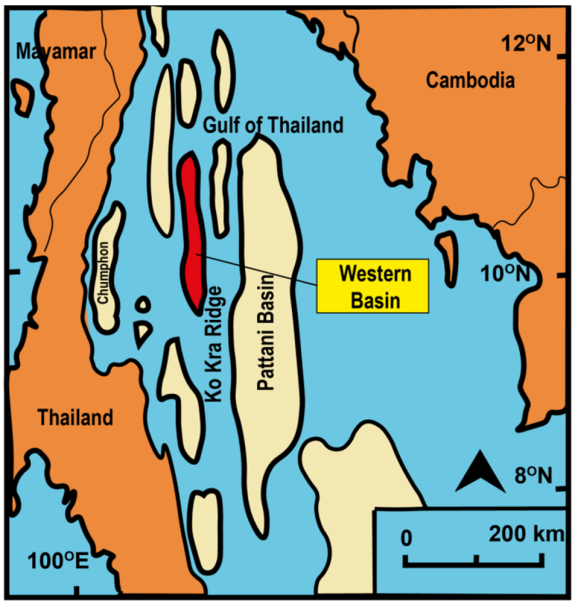

Figure 1. Map shows the location of the study area located in Western Basin, Gulf of Thailand.

4. Data Sets

Well log Data

There are 11 exploration wells located in the study area. The original well log data consists of gamma ray, neutron porosity, density, and resistivity. Only 10 wells have compressional sonic logs, and shear sonic logs occur at 8 wells. Check shot data are available in 7 wells and were used in well-to-seismic correlation as an original time-depth function.

Seismic Data

The study used approximately 460 km^2 of 3D seismic data, which ranged from 0 to 6 seconds. There are four 3D post-stacked time migration (PSTM) volumes used in this study. The first volume is a full-stacked volume. The second to fourth volumes are three partial-angle stacked volumes. The three partial-angle stacked seismic data are near- (10˚- 20˚), far- (30˚- 40˚), and very far- (40˚-50˚) angle stacked seismic. The reservoir target ranges from 0.85 to 1.5 seconds. The dominant frequency of the target interval is around 30 Hz.

5. Methodology

The methodology that was used in the study can be divided into three stages: rock physics analysis, seismic inversion and seismic attributes analysis. The result from rock physics analysis is to understand the behavior of both lithology and fluid as a function of rock type, fluid content, reservoir quality and depth.

Rock Physics Analysis

The well log data of 10 wells drilled in the study area were used in the rock physics analysis. The aim is to determine which rock properties that best discriminate lithology and fluids within the reservoir interval. The rock properties which are transformed from the well log data will be integrated with the seismic volume to convert it into an inverted elastic impedance volume. Part of the analysis is to generate several cross plots using density (ρ), P-wave velocity (Vp), S-wave velocity (Vs), P-impedance (Z) and elastic impedance (EI) with respect to shale volume (Vshale). Depth was also used as a function in the cross plots to observe the depth dependence of rock physical parameters. Compressional velocity (P-wave or Vp) and density (ρ) were combined with the extracted wavelet to calculate the acoustic impedance or P-impedance (Z). P-impedance is linked to a normal incidence (vertical) reflection.

Elastic impedance is a generalization of acoustic impedance for variable incidence angle. Elastic impedance provides a consistent and absolute framework to calibrate and invert non zero-offset seismic data just as AI does for zero-offset data. This elastic impedance is a function of P-wave velocity, S-wave velocity, density, and incidence angle. The elastic impedance (EI) from different reflected angles was computed using Connolly equation, 1999.The middle value of each partial-angle stack seismic (near -15˚, far -35˚, and very far -45˚) was used as an input value of reflected angle to compute the elastic impedance logs.

Colored Inversion

Colored inversion is a modification of Recursive Inversion, basically trace integration, achieved by applying a special filtering technique in the frequency domain. The amplitude spectrum of the well log is compared with that of the seismic data. An inversion operator is designed that brings the seismic amplitudes of the frequencies in correspondence with that seen in the well. The operator phase is -90 degrees. This operator is then applied to the whole seismic cube.

Seismic Attributes

RMS (Root Mean Square)

The RMS amplitude is a post-stack attribute which computes Root Mean Squares on instantaneous trace samples over a specified window (Petrel Help). This attribute can be useful when run with sample values which have positive and negative domains like in seismic traces. The time window for the RMS is determined by the thickness of the target interval such as sands.

Sweetness

The Sweetness is a response attribute which is an implementation of two combined attributes (Envelope and Instantaneous Frequency) and is used for the identification of features where the overall energy signatures change in the seismic data (Petrel Help). Sweetness is defined as response amplitude divided by the square root mean of response frequency. This attribute also is designed to identify "sweet spot", places that are oil and gas prone (Barnes, 2016).

6. Result and Interpretations

6.1 Rock Physics Analysis

To understand the behavior of the rock properties, shale volume was used to differentiate sand and shale to see if their response is depth-dependent. Several cross plots were created from well data such as density, P-wave velocity, and P-impedance versus depth, color coded by the shale volume (Figure 2a – 2c). The shaly sand values were not plotted in order to analyze only the clean sand and pure shale trends. The feature highlighted in yellow represents reservoir Sand A. The cross plots show that the values of these parameters increase with depth, following the compaction trend. Sands characters are lower density, lower P-wave velocity, and higher S-wave velocity than shales.

According to the cross plots, the density shows a strong contrast between sand and shale trend at all depths, because the density of sand is everywhere significantly lower than that of shale. A higher contrast characterizes the shallower section and becomes a lower towards the deeper section. Based on the density cross plots, the highest density in Sand A are interpreted to be shale, followed by shaly sand and clean sand as the lowest density value.

The P-wave velocity versus depth cross plots indicate a dependency on both lithology and depth. P-wave velocity of sand in Sand A is lower than shales down to 1300 meters. Below that depth, the P-wave velocity of sands is similar to shales and show as an overlap, and below 1300 meters the sand trend and shale trend are exchanged and result in a cross over pattern. But, overall the general trend of sand and shale were almost the same in both P-wave and S-wave which caused a narrow contrast. The computed P-impedance shows a small contrast of sand and shale trend, due to the effect of the P-wave velocity. This rock property trend refers to the density and P-wave velocity, since it is a combination of these two logs. The cross plot shows that P-impedance of sand is lower than shale in Sand A, but the contrast of these two lithology trend becomes lower as depth increases. Therefore, the P-impedance can be used to discriminate sands from shales clearly in Sand A or shallow part of Sequence T4.

The cross plots of near-, far-, and very far- angle elastic impedance logs versus depth with respect to shale volume show various contrasts in Figure 2 (d-f). The near-angle elastic impedance shows a quite similar lithology trend with the P-impedance. However, the far-angle elastic impedance shows a strong contrast compared to the near-angle elastic impedance and P-impedance. The far-angle elastic impedance of sands is significantly lower than shales compared to the near-angle elastic impedance and P-impedance. This results in clearly separated trends of sands and shales for the whole interval. The near-angle elastic impedance shows almost overlap zones of sand and shale. In addition, the far-angle elastic impedance shows a similar trend with very far-angle elastic impedance, although the far-angle elastic impedance still shows a stronger contrast.

Based on the cross plots results in Figure2, the P-impedance that is generated using full-stacked seismic volume can only resolve lithology discrimination to a certain depth, in the shallow stratigraphic interval. At a higher depth, the full stacked seismic volume shows some limitation in defining lithology trend in the study area. Unlike the P-impedance, the far-angle elastic impedance shows a better contrast between sand and shale trend at all stratigraphic intervals. Therefore the applied inversion technique will use the far-angle elastic impedance volume.

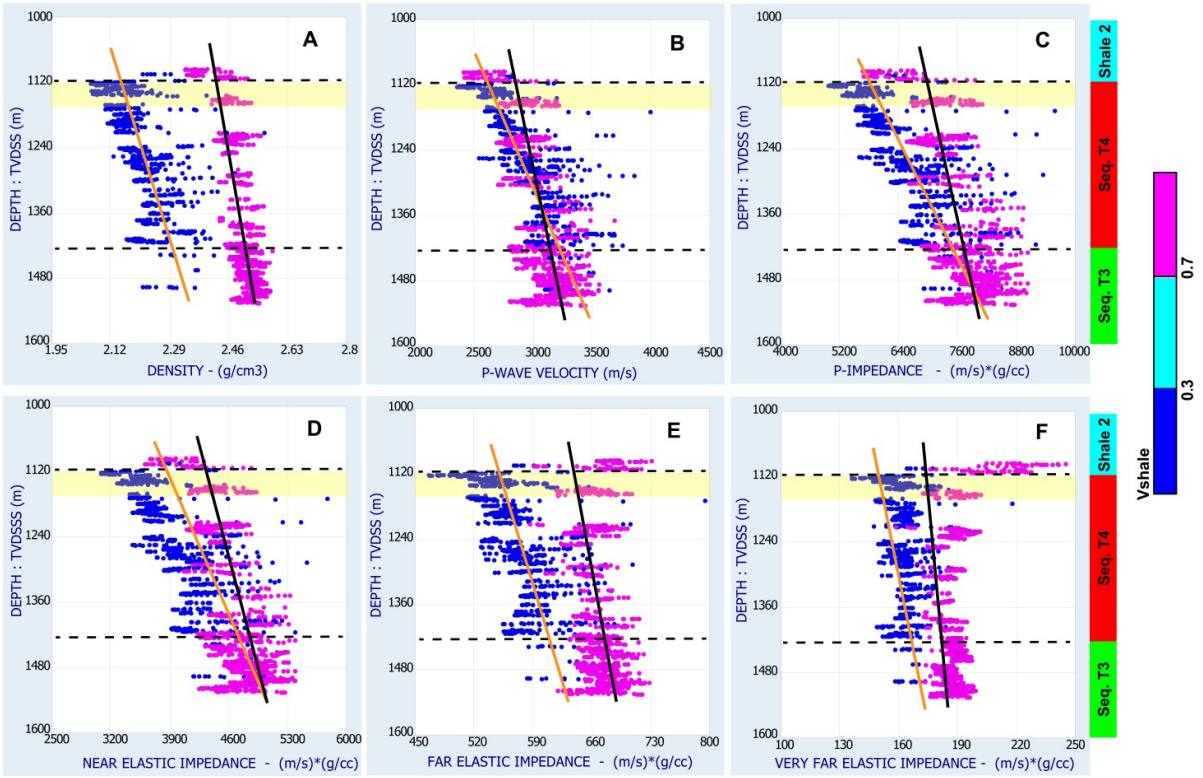

Figure 2. Well log data cross plots (well CU-9) of density, P-wave velocity, P-impedance, near-angle E-impedance, far-angle E-impedance, and very far-angle E-impedance versus depth color coded by the shale volume. The black dash lines are Top of Sequence T4 and Top of Sequence T3. The black lines are fitted with the data point of pure shale (shale volume > 0.7). The orange lines are fitted with the data point of sand (shale volume < 0.3).

6.2 Wavelet Estimation and Well-to-seismic Correlation

Prior to doing the inversion analysis, checkshot correction of the P-wave sonic log to match with the two-way travel time of the seismic was completed. Next, the well data were tied to the seismic to obtain the correct P-wave sonic at the well location. Wavelets were extracted from the partial-angle stacked seismic and well data composed of sonic and density logs were used to generate the synthetic seismograms. The synthetics of seven wells were created in the study area.

The sea bed horizon was mapped in the study area as a strong trough seismic reflector that refers to the negative polarity of seismic data. The top sands from the synthetic seismogram were displayed as peak reflection and these reflections were used to match with the peak of seismic data. According to the synthetic trace and seismic trace process, the seismic volumes are suggested as being zero phase or close to zero phase. Therefore, the wavelets were extracted from near-angle stacked and far-angle stacked seismic data at constant phase with phase rotation of zero-offset. These wavelets were extracted from the target interval between Top Sand B to Top of Ratburi Basement using the seismic data. These wavelets are called statistical wavelet which extracts frequency from a time window between 850 and 2124 milliseconds.

The study area data base included S-wave velocity logs in eight wells. These wells were integrated with the near-angle (15˚) and far-angle (35˚) traces to generate synthetic seismogram for each partial-angle elastic impedance. The extracted statistical wavelets were used to convolve with the reflection coefficient constructed from the well log data to create synthetic seismograms for each angle.

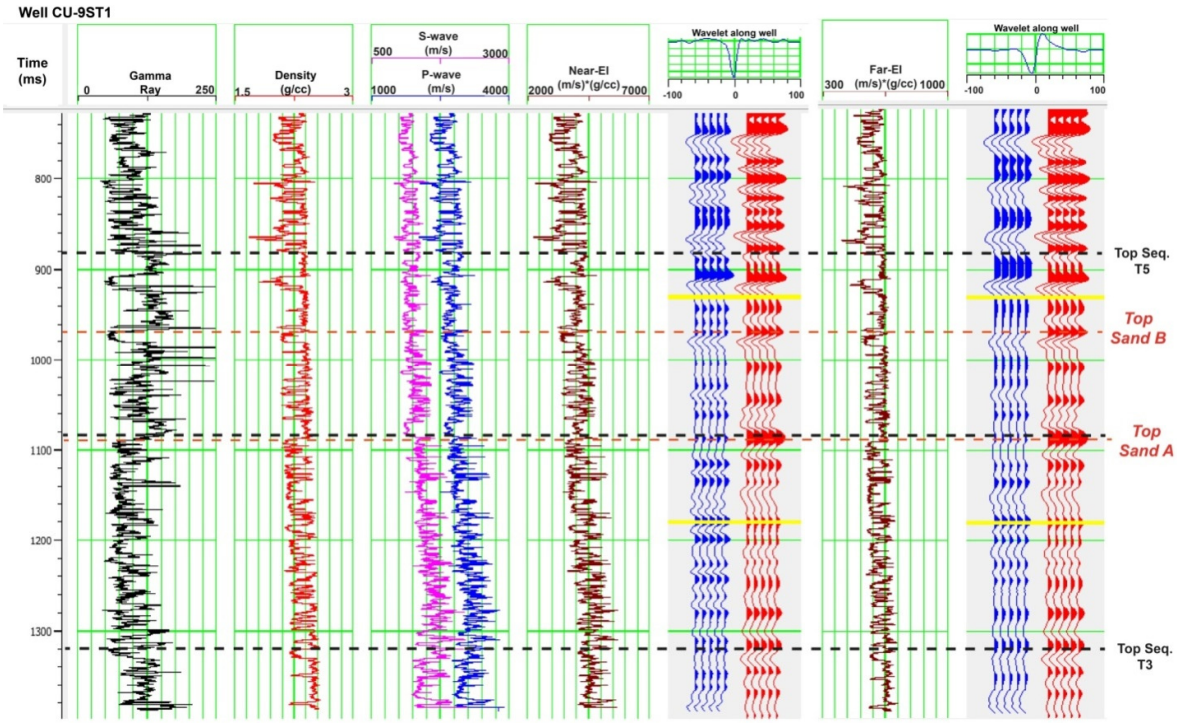

Figure 3. Synthetic Seismogram of well CU-9ST1 which is calculated at 15 degree and 35 degree were compared with the near-angle and far-angle stack seismic. The computed elastic impedance at near-angle (15˚) and far-angle (35˚) were compared with the synthetic seismograms and other well log data. The matched event is marked by dash line at top sand and marker sequence.

To improve the correlation coefficient between well-to-seismic tie and to provide a more reliable final time-depth function, the new wavelets were extracted using the wells data. These averaged wavelets were extracted from ten wells at constant phase. The correlation coefficient value from the well-to-seismic tie using these extracted wavelets ranges from 0.5 to 0.9. The result of the well-to-seismic-tie of well CU-9ST1 is shown in Figure 3. These wavelets will be used later in the seismic inversion process.

However, the synthetic does not match with the seismic data since the correlation coefficient values are quite low, although in some wells there are high values of correlation coefficients. The low value of correlation coefficient can lead to mismatches of the well data to the seismic volumes. Since these synthetic will be an input to the seismic inversion process, therefore mismatch of this process will cause inaccurate inversion analysis and affect the results of the inverted volumes. There are several reasons which caused the poor well-ties, for instance wrong input of checkshot data, bad checkshot values, well location problems, error in seismic migration, spatial sampling, and different propagation paths for sonic and seismic or deviated wells.

6.3 Horizon and Fault Interpretation

Based on the well marker, Top Sand A was defined in all wells and Horizon Sand A was interpreted on the seismic data. According to the rock physics analysis and well-to-seismic tie, the far-angle elastic impedance shows a strong contrast between sand and shale. Therefore, this horizon was mapped using the far-angle stacked seismic volume. Horizon Sand A was picked at strong peak (blue) seismic reflector and characterized by good continuity reflection and strong amplitude (Figure 4).

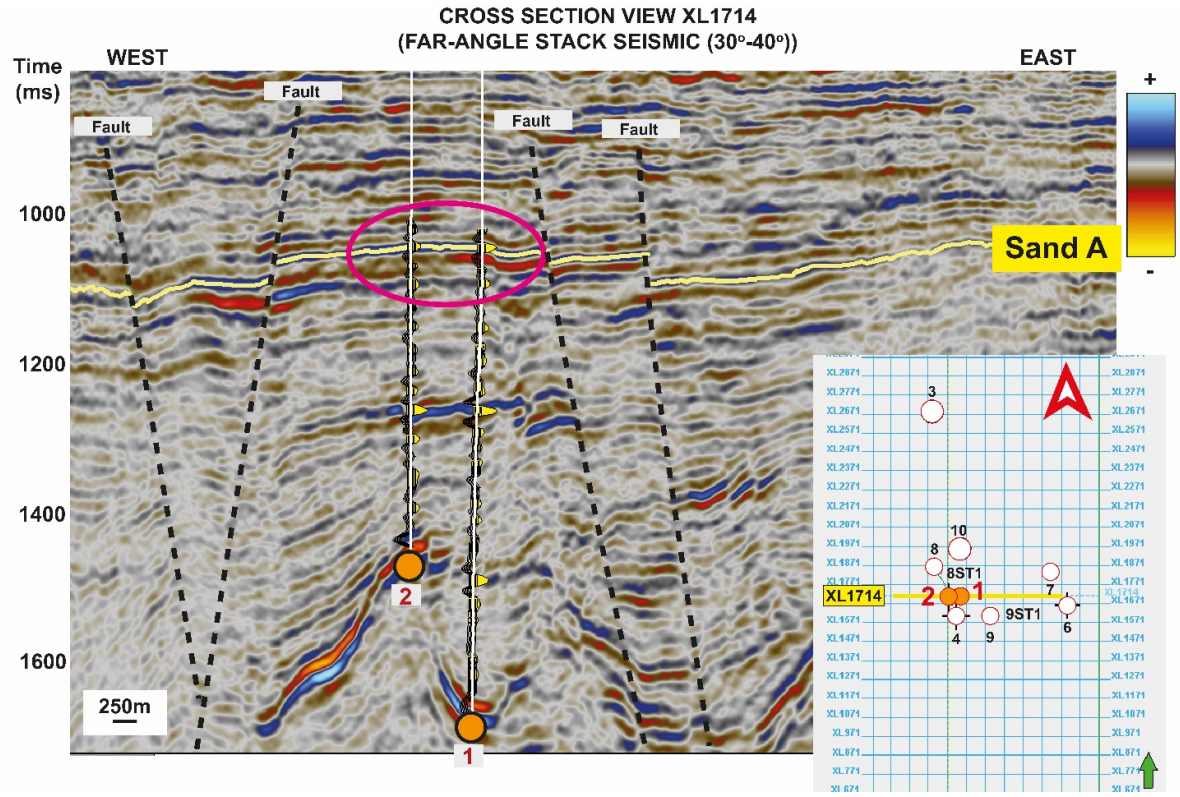

Figure 4. Cross-section of well CU-1 and CU-2 which shows Horizon Sand A picked on far–angle stacked seismic and synthetic seismogram (in pink circle) along the wellbores.

Horizon Sand B within Sequence T5 was created using a phantom horizon around 100 milliseconds above Horizon Top Sand A, since the reflection of this sand is not as continuous as Horizon Sand A.

6.4 Elastic Impedance Inversion

6.4.1) Initial Low Frequency Model

Seismic data are band-limited with no low frequencies information. Quantitatively, low frequency data is very vital in predicting fluid content, porosity and other rock properties. Information from the low frequency will affect the geological interpretation of the inverted impedance traces. Since the well logs are broadband and contain low to very high frequency information, well logs were used to provide the low impedance information which is missing from the seismic data. Seven wells were chosen to build the initial low frequency model for the near-angle and far-angle stacked seismic volumes respectively. These models are acquired from the computed elastic impedance logs at 15˚ (near-angle) and 35˚ (far-angle).

6.4.2) Inversion Analysis

The near- and far-angle elastic impedance inversion models were created by using the colored inversion method. In this process, a single operator with -90 degrees phase shift was applied to the seismic trace to transform it directly into the inversion result. The low frequency trend from the wells was applied in the process, therefore the impedances are absolute and the output seismic impedances can be correlated with log impedances. The exported output models were set to sampling rate at 2 milliseconds (two-way time).

The inverted elastic impedance logs created from the seismic volumes along wellbore were compared to the original elastic impedance log which was then re-sampling to be at the seismic scale. The resulting comparison between original logs, initial model, and

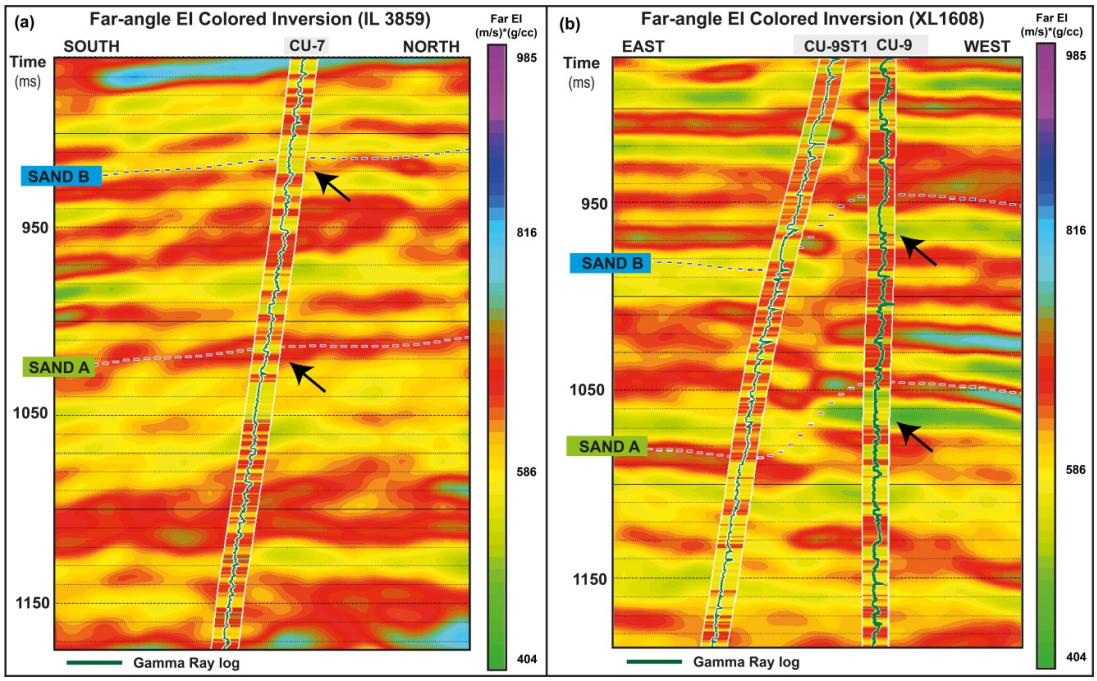

Figure 5. Cross-section of inverted far-angle elastic impedance along well CU-7 (blind-test well) (a) and along well CU-9 and CU-9ST1 (b) within Sequence T5 to T3.

inverted logs show the correlation coefficient ranges from 0.58 to 0.63. This lower than expected correlation may be due to an original poor well-to-seismic tie as mentioned before.

6.4.3) Comparison of Elastic Impedance Inverted Volume with Blind-Test Wells

The well log data and inverted elastic impedance volumes were compared with the well CU-7 that was not used in the inversion process. According to the rock physics analysis, the elastic impedance of sand is lower than shale, and is represented by green to yellow colors. The low far-angle elastic impedance aligns better with the low gamma ray log of the well than the low near-angle elastic impedance (Figure 5). The blind-test well which was not used in the inversion process shows unconformable results for both near-angle and far-angle elastic impedance inversion for Sand A and Sand B. This mismatch can be due to low synthetic quality and poor inversion analysis. However, it shows conformable results of near-angle and far-angle elastic impedance inversions in Sand A and Sand B at the wells, which were used to build the inversion model based on well log interpretation

The far-angle elastic impedance inversion shows a more detailed image of sand and shale, and possible oil-bearing sand than the near-angle elastic impedance inversion. The green color in well CU-9 which may indicate oil-bearing sand of Sand A was seen clearly in the inverted far-angle elastic impedance. Whereas, the inverted near angle-elastic impedance only shows a subtle green color. However, since the inversion analysis correlation is lower due to the poor synthetic results, this may lead to inaccurate inverted volumes in the other wells. Therefore the workflow for the inverted volumes was not continued in this study.

6.5 Seismic Attributes

6.5.1) RMS Amplitude Attribute

RMS amplitude attribute was applied to the target interval Sand A and Sand B in each partial-angle stacked data (near-, far- and very far-angle) in order to identify the sand reservoir distribution in the study area.

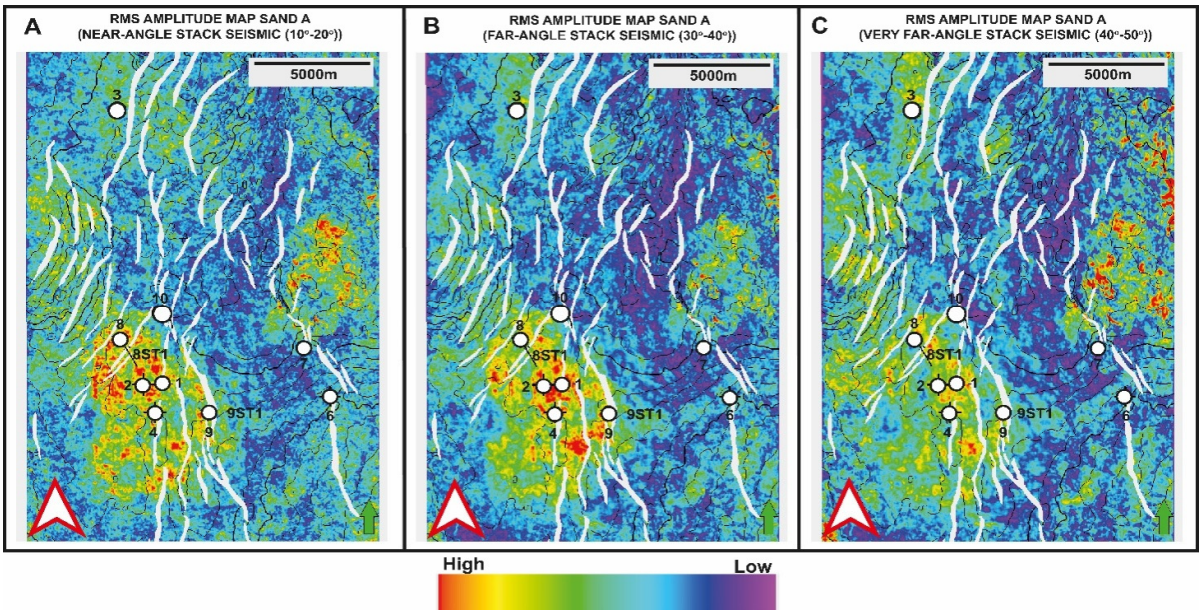

Figure 6. The RMS amplitude map of Sand A in each partial-angle stacked seismic. Near-angle (a), far-angle (b), and very far-angle (c) stacked seismic data.

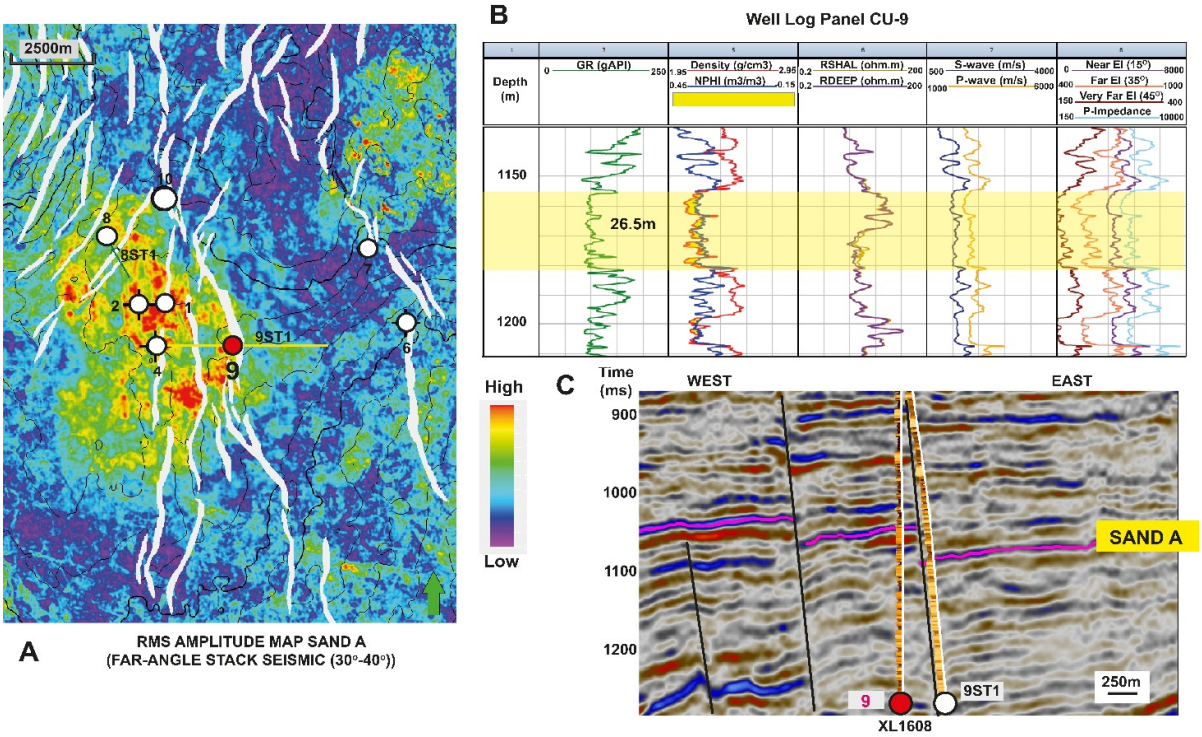

Figure 7. The (zoom-in) RMS amplitude map of Sand A in far-stacked seismic data (A), the well log panel shows the RMS window range (orange zone) covered in well CU-9 (B), and seismic section (XL1608) along the well bores CU-9 and CU-9ST1 (C).

Using the information from the rock properties analysis, the far-angle shows a stronger contrast of sand and shale trends than the near-angle and very far-angle elastic impedance. Consequently, the far-angle stackedseismic

displayed a better image of amplitude contrasts between sand and shale (Figure 6).

The high amplitude valueon the RMS amplitude map can be indicating sand at the well locations andit can be observed mostly in the center part where the wells are located within the high structural closure. These high amplitudes indicate sand distribution in the study area whichwas confirmed with the well log data of well CU-9, where dominant thick sand bodies were found in the well (Figure 7).

In general, the geometry of channel-like features of both Sand A and Sand B were quite difficult to see in the study area, this could be caused by the depositional environment of these sands as being mainly in a braided fluvial environment which is comprised of amalgamated channel sand bodies.

6.5.2) Sweetness Attribute

The sweetness attribute was also applied to the near-, far-, and very far-angle stacked seismic data to identify the hydrocarbon zones in the study area. Figure 8, shows time slice along the reservoir Sand A at 1.05 seconds. According to the map, the high value of sweetness can be seen better in the far-angle stacked seismic. The sweetness spot is indicated with bright yellow to red color. These sweet spots can mean that the area is probably saturated with hydrocarbon or there is a big acoustic impedance contrast between sand in the channel with shale around the channel. Figure 9showsthe sweetness attribute in cross-section view along the well CU-9 and CU-9ST1 in each partial-angle stacked seismic data. The far-angle stacked seismic shows stronger high sweetness values than near-angle and very far-angle stacked seismic data. The well log data of well CU-9 confirmed there is multiple stacked oil sand from sequence T5 to Sequence T4, including the Sand A.

The sweetness was compared with the RMS attribute to help identify the hydrocarbon-bearing zones. This will represent the hydrocarbon distribution at the time of seismic acquisition 2010. Comparison between these attributes can indicate whether the anomalies are due to sand distribution only or indicate hydrocarbon zones. The sweetness map of Sand A displayed a more focused area of high values of sweetness (in red color) than the RMS amplitude map. Therefore, the sweetness map can be an indicator of possible hydrocarbons in the study area.

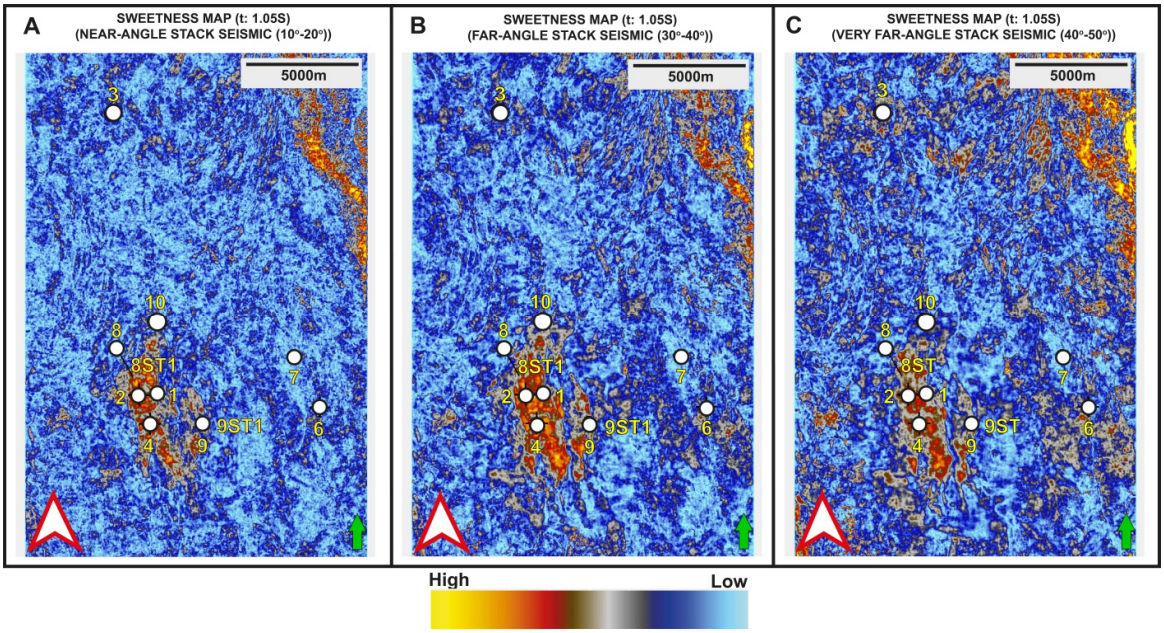

Figure 8. The Sweetness attribute map at time slice 1.05 seconds along Horizon Sand A. Near-angle (a), far-angle (b), and very far-angle (c) stacked seismic volume.

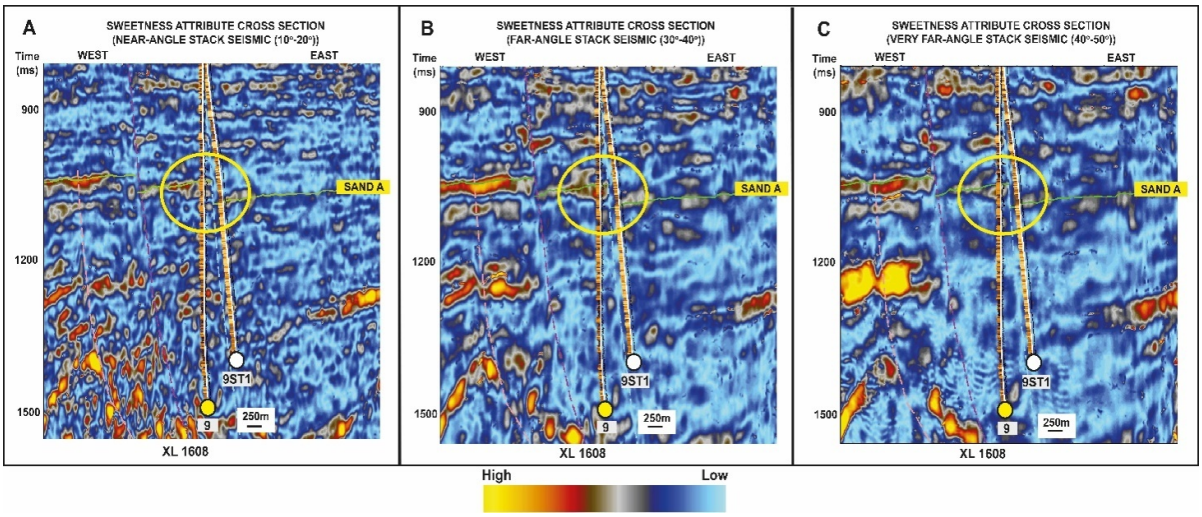

Figure 9. Cross-section of sweetness attribute (XL1608) showing Horizon Sand A along wellbore CU-9 and CU-9ST1 at time 1.05 seconds in each partial-angle seismic. Near-angle (a), far-angle (b), and very far-angle (c) stacked seismic volume.

7. Discussion

According to the elastic impedance and seismic attributes results, there are several points obtained from this study, which reveal the main advantages using far-offset seismic volumes information. All points are summarized below;

a) The far-angle stacked seismic data gives more reservoir properties information than near-angle stacked seismic and very far-angle stacked seismic data.

b) According to the rock physics analysis, the P-impedance shows a limitation in discriminating the sand and shale in the study area, due to the similar value of P-wave velocity. However, the rock properties of the elastic impedance show that it is a good technique to discriminate the lithology trend, especially the far-angle elastic impedance. The greater the incident angle (larger offset), makes the density become more dominant than near-angle stacked seismic.

c) The inverted far-angle stacked seismic data is confirmed to be a good technique to predict the lithology and possible fluid type in the study area. However, the low quality of the synthetic makes the inversion analysis to be poor and the resulted inverted volume in the study area to be inaccurate. Therefore, the inversion process will not be discussed in more detailed.

d) The RMS amplitude can be used to identify reservoir distribution of Sand A and Sand B. Moreover, the sweetness attributes can be used to predict hydrocarbon-bearing sand in the study area. The geometry of sand body on the RMS amplitude maps is more extensive than on the sweetness attribute maps. The distinct geometry between these attribute can indicate hydrocarbon presence which affect the frequency absorption of the sweetness attribute in the study area. However, the 'sweet-spot' in the study area is quite subtle, since reservoir in the study area is comprised of amalgamated sand bodies.

e) The far-angle stacked seismic data gives a better image of mapping the sand distribution in RMS and sweetness attributes. The sweetness map also displayed hydrocarbon-bearing zones better in far-angle stacked seismic data. This aligned with the rock properties analysis where far-angle elastic impedance shows strong contrast of sand and shale, unlike the near-angle and very far-angle elastic impedance, and can be used to identify the lithology.

8. Conclusions

The rock physics analysis, post-stack inversion and seismic attributes techniques were applied to the data set of the study area in the Western Basin, Gulf of Thailand. The results are elastic impedance inversion and seismic attributes using far-offset is ideal techniques to apply in the data set in order to enhance prediction of reservoir distribution and fluid type. The conclusions are summarized below;

- Density can be used to discriminate the lithology in all sequences, while P-wave velocity shows some overlap zones of sand and shale at certain depths within the same stratigraphy sequence.
- Far-angle elastic impedance can differentiate sand and shale in Sand A and Sand B clearly, while P-impedance and near-angle elastic impedance has limitations in distinguishing the lithology due to the trend value of P-wave velocity between sand and shale being similar.
- Far-angle elastic impedance inversion can be used to identify the reservoir sands better and more detailed than near-angle elastic impedance inversion. The far-angle elastic impedance inversion could be a good technique to identify reservoir distribution to help minimize the exploration risk and maximize development potential.
- High amplitude values on RMS attribute represents the distribution of reservoir sand and high values on sweetness attribute represent the oil-bearing sand. Thus, the sweetness attribute can be used as a direct hydrocarbon indicator when compared with the RMS attribute.

9. Acknowledgements

I would like to express my gratitude to my thesis supervisor Mr. Angus John Ferguson for his valuable guidance, patient support, and encouragement throughout this research work. I would like to thank Professor John Warren and Associate Prof. Dr. Thasinee Charoentitirat for their knowledge through the Petroleum Geoscience Program.

This thesis was made possible through academic and financial support from the PTT Exploration and Production for the opportunity and scholarship for studying Master Degree of Petroleum Geoscience at Chulalongkorn University.

10. References

Barnes, A.E., 2016, Hanbook of Poststack Seismic Attributes: SEG Geophysical References Series, no. 21, p. 59.

Connolly, P., 1999. Elastic Impedance: The Leading Edge, v. 18, p. 438-452.

Heward, A.P., Chuenbunchom, S., Makel, G., Marsland, D., Spring, L., 2000, Nang Nuang oil field, B6/27, Gulf of Thailand: karst reservoirs of meteoric or deep-burial origin?: Geological Society of London, v. 6, no. 1, p. 15-27.

Kamolsilp, M., 2016, Elastic Impedance Inversion for Reservoir and Hydrocarbon Identification, Northern Pattani Basin, Gulf of Thailand: M.Sc. thesis, Chulalongkorn University, 54 p.

Khanna, M., Comrie-Smith, N., Lawlor, M., and Virdy, M.K., 2013, Bualuang Oilfield, Gulf of Thailand: A Successful Development Using Geosteered Horizontal Wells: adapted from oral presentation, AAPG International Conference and Exhibition, Singapore, 2012.

Lain, H.M., and Bradley, K., 1987, Exploration and development of natural gas, Pattani Basin, Gulf of Thailand: Transactions of the fourth circum-Pacific energy and mineral resources conference, Singapore, p. 171-181.

Mukerji, T., Jorstad, A., and Mavko, G., 1998, Near and far offset impedance: Seismic attributes for identifying lithofacies and pore fluids: Geophysical Research Letters, v. 25, no. 24, p. 4557-4560.

Tang-On, A., 2018, The use of inversion volumes for reservoir imaging, CU Field, Gulf of Thailand: M.Sc. thesis, Chulalongkorn University, 42 p.